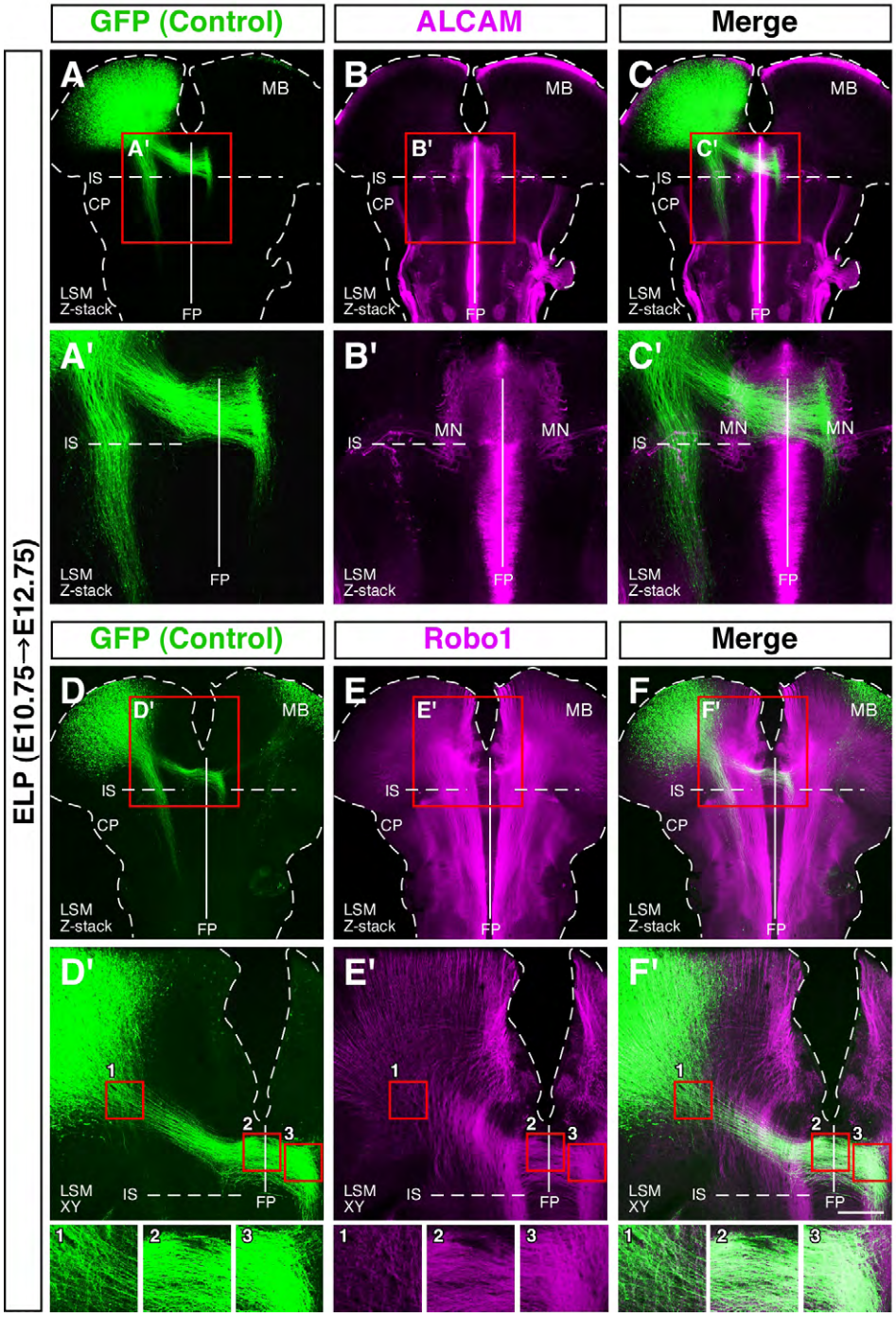

Fig. S1. Trajectory of midbrain commissural axons and the expression pattern of Robo1.

(A-F') GFP-expression vector was electroporated into the dorsal midbrain (MB) at E10.75, and the trajectory of GFP-labeled axons was analyzed in flat-mounted preparations at E12.75, together with immunostaining for expression of ALCAM (B,B') and Robo1 (E,E'). (A-C) Z-stack images of 26 optical sections (10 μm thickness) obtained by confocal LSM. (A'-C') High power views of red rectangles in (A-C), respectively, but showing Z-stack LSM images of 31 optical sections (5 μm thickness). ALCAM staining delineates the location of the floor plate (FP) and oculomotor neurons (MN) in the ventral midbrain. GFP-labeled commissural axons grow caudally in the region between the floor plate and oculomotor neurons on the contralateral side. (D-F) Z-stack images of 25 optical sections (10 μm thickness) obtained by confocal LSM. (D'-F') Higher magnification views of red rectangles in (D-F), respectively, but showing an XY-plane of LSM image. Numbered small red boxes in (D'-F') indicate areas enlarged in corresponding insets below. As midbrain commissural axons grow ventrally toward the floor plate, Robo1 expression on these axons is gradually upregulated. Crossing and post-crossing segments of these commissural axons seem to express higher level of Robo1 compared with the pre-crossing segment. IS, isthmus; CP, cerebellar plate. Scale bar: 600 μm in A-F; 240 μm in A'-F'.

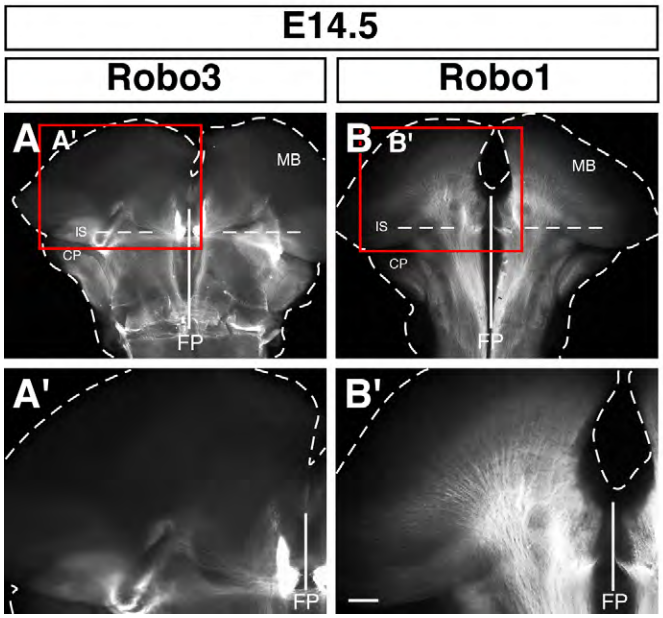

Fig. S2. Expression of Robo3 and Robo1 in the mouse midbrain at E14.5.

(A-B') Immunohistochemical localization of Robo3 and Robo1 in E14.5 flat-mounted preparations. (A,A') Robo3 expression on pre-crossing segment of midbrain commissural axons is downregulated at this stage. (B,B') Expression of Robo1 is still maintained on midbrain ipsilateral axons. (A',B') High power views of red boxes in (A,B), respectively. Scale bar: 500 µm in A,B; 250 µm in A',B'.

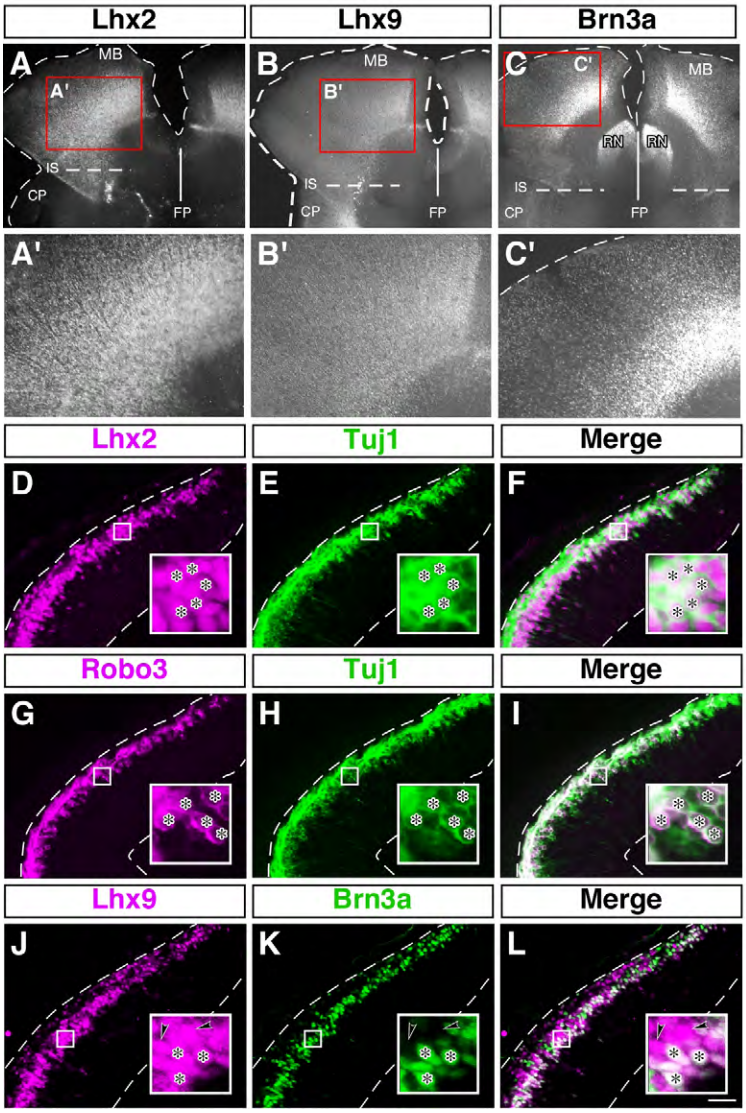

Fig. S3. Expression of transcription factors and Robo3 in the dorsal midbrain.

(A-C') Expression of Lhx2, Lhx9, and Brn3a in flat-mounted preparations at E11.5. (A'-C') High power views of red rectangles in (A-C), respectively. Lhx2 and Lhx9 are selectively expressed in the dorsal midbrain. Brn3a is also expressed in the area where Lhx2 and Lhx9 are expressed. Ventral midbrain cells positive for Brn3a correspond to red nucleus neurons (RN). (D-I) Double-immunostaining analyses for expression of Lhx2/Tuj1 (D-F) and Robo3/Tuj1 (G-I). Lhx2 and Robo3 are expressed by postmitotic neurons, as judged by the expression of Tuj1. Asterisks represent postmitotic neurons expressing Lhx2 and Robo3, respectively (insets). (J-L) Double immunolabeling of Lhx9 and Brn3a in transverse sections of the dorsal midbrain. Similar to the expression of Lhx2 (Fig. 3D-F'), a subset of Lhx9-positive cells expresses Brn3a. Asterisks indicate cells double-positive for Lhx9 and Brn3a, and arrowheads depict Lhx9-positive/Brn3a-negative cells (insets). Small boxes in (D-L) indicate regions enlarged in insets. Scale bar: 250 μm in A-C; 100 μm in A'-C'; 50 μm in D-L.

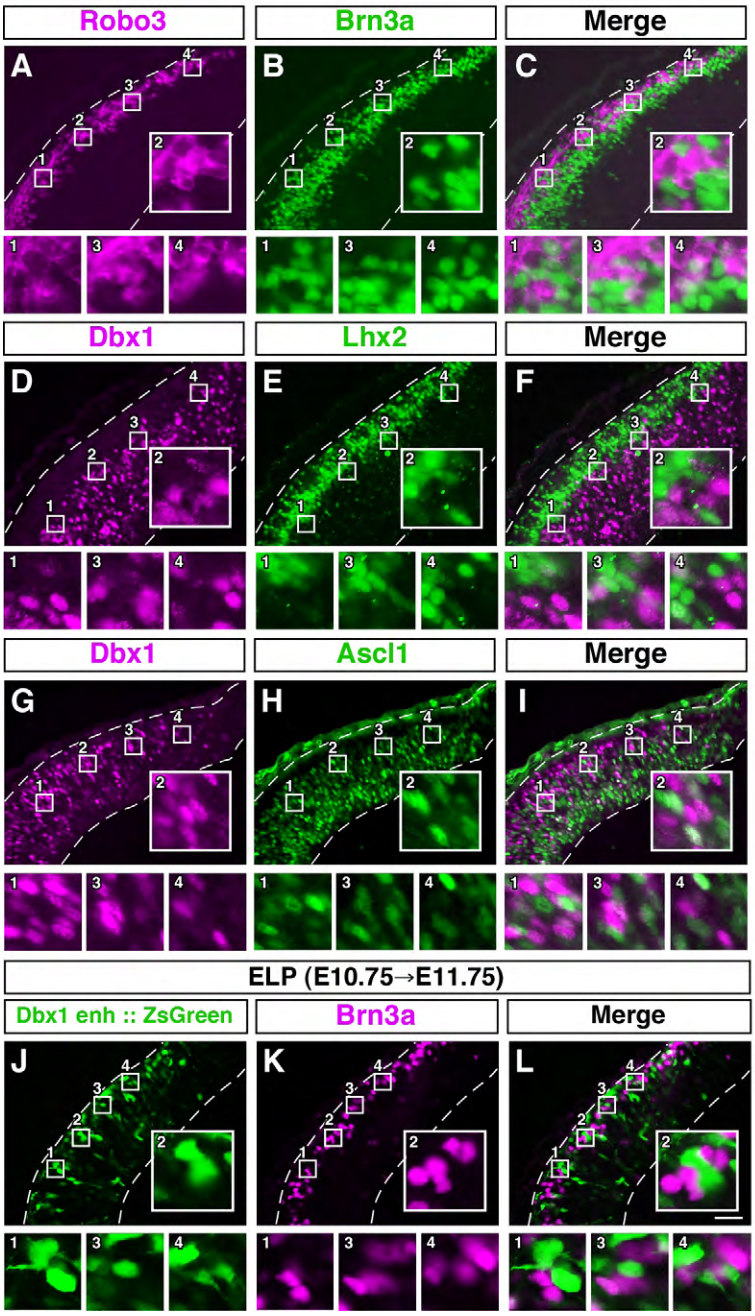

Fig. S4. Detailed expression analyses of transcription factors and Robo3 in the dorsal midbrain.

(A-I) Expression of Brn3a, Dbx1, Lhx2, Ascl1, and Robo3 in transverse cryosections of E11.5 dorsal midbrain. (A-C) Double immunolabeling of Robo3 and Brn3a, showing Robo3-positive cells are segregated from Brn3a-positive cells. (D-F) Dbx1-positive cells do not express Lhx2. (G-I) Dbx1-expressing cells are segregated from Ascl1-positive cells. (J-L) Cell-lineage tracing analyses using *Dbx1*-enhancer element. *In vivo* electroporation of *Dbx1 enhancer::ZsGreen* vector was carried out at E10.75, and the expression of ZsGreen and Brn3a was analyzed in transverse sections at E11.75. ZsGreen-positive cells do not express Brn3a. Numbered small boxes in (A-L) indicate areas enlarged in corresponding insets below. Scale bar: 50 μm.

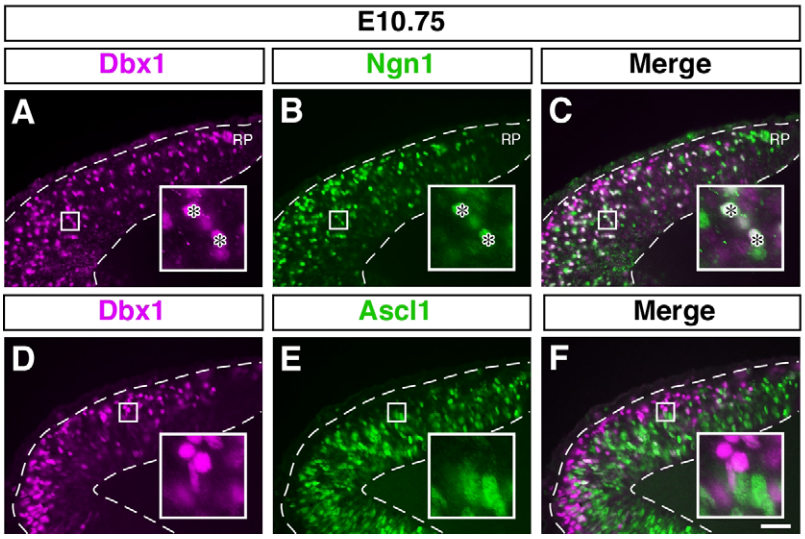

Fig. S5. Expression pattern of Dbx1 in the dorsal midbrain at E10.75.

(A-F) Expression analyses of Dbx1, Ngn1, and Ascl1 in transverse sections of the dorsal midbrain. (A-C) Dbx1 is expressed in subsets of Ngn1-positive progenitors. Asterisks in insets show cells double-positive for Dbx1 and Ngn1. (D-F) Dbx1-positive cells do not express Ascl1. Small boxes in (A-F) indicate areas enlarged in insets. Scale bar: 50 μm. Note that the expression profile and the location of Dbx1-positive cells are basically similar to those observed at E11.5 (Fig. 4). In this study, we show in control embryos that *GFP* plasmids can be successfully targeted into commissural neurons by *in vivo* electroporation at E10.75 compared to E11.5 (Fig.1). Because the overall localization pattern of Dbx1-positive cells is similar between E10.75 and E11.5, it is unlikely that the migration of Dbx1-positive cells away from the ventricle is a direct cause that yields a dramatic difference of the *GFP*-transfection efficiency into commissural neurons. Rather, we reason that, like the case of the relationship between birthdate and laminar fate in the cerebral cortex (Leone et al., 2008, Curr. Opin. Neurobiol. 18, 28-35), a change in the competence of neural stem cells to produce certain progenitor cells committed to express Dbx1 may be involved in the difference of the *GFP*-transfection efficiency.

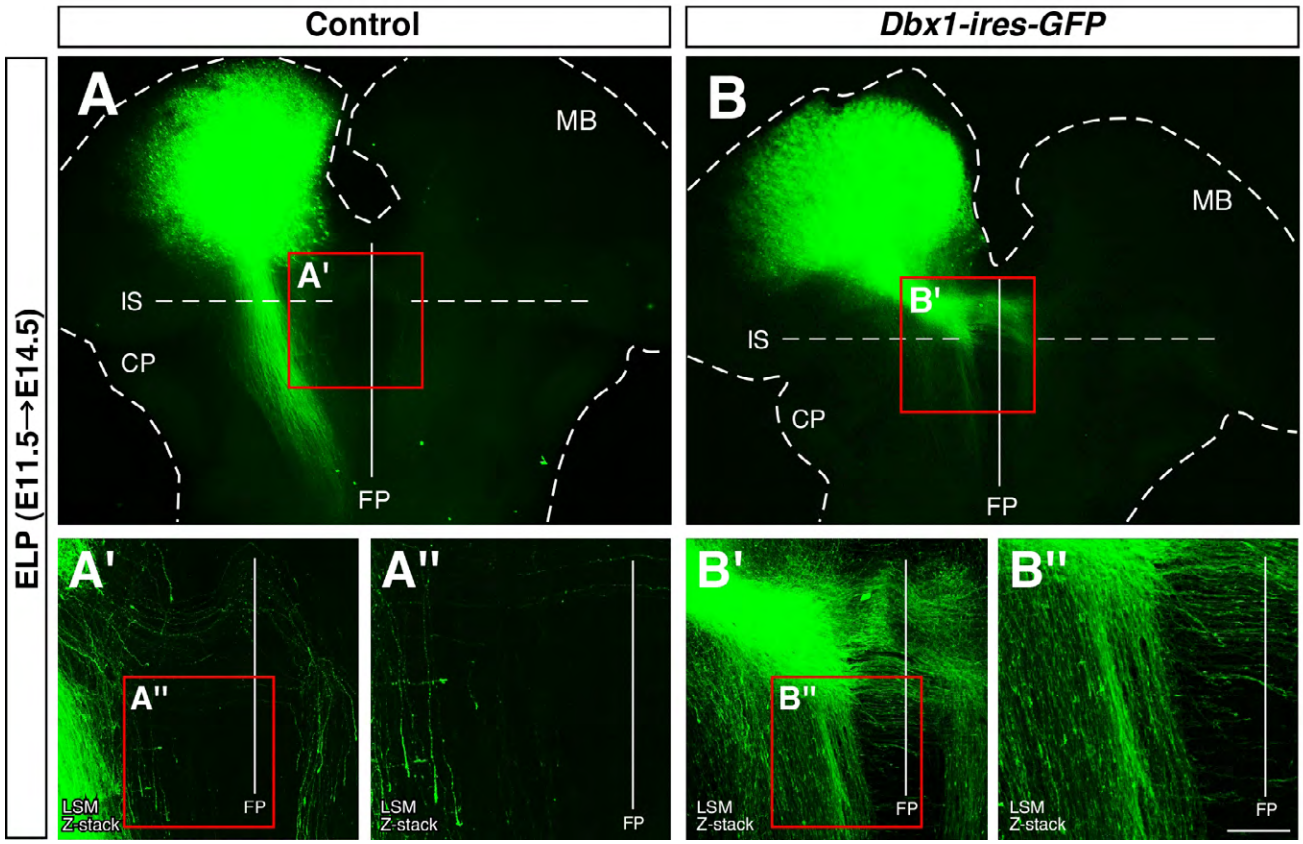

Fig. S6. Change in pathfinding behavior of ipsilateral axons by Dbx1 misexpression.

(A-B") Trajectory of GFP-labeled axons observed in flat-mounted preparations. Electroporation was performed at E11.5, and the axon pathfinding was analyzed at E14.5. (A,A',A") The majority targeted by *GFP* electroporation at this stage are ipsilateral axons (see also Fig. 1C,C'). (A',A") High power views of red rectangle in (A,A'), respectively, but showing a Z-stack image of 35 optical sections (5 µm thickness) obtained by confocal LSM. (A") In controls, ipsilateral axons grow caudally at a distance from the floor plate (FP). (B,B',B") Electroporation of *Dbx1* (*Dbx1-ires-GFP*) at E11.5 causes changes in pathfinding behavior of ipsilateral axons. (B') Pathfinding phenotypes of ipsilateral axons triggered by Dbx1 misexpression. As also shown in Figure 6 (Fig. 6B,B'), midline crossing is dramatically induced. (B") Midline-approaching phenotype represented by a behavior of ipsilateral axons that make a caudal turn at more ventral locations, followed by caudal growth closer to the FP compared with control (A"). (B',B") Higher magnification views of red rectangle in (B, B'), respectively, but showing a Z-stack image of 42 optical sections (5 µm thickness) captured by confocal LSM. Scale bar: 450 µm in A,B; 200 µm in A',B'; 100 µm in A",B".

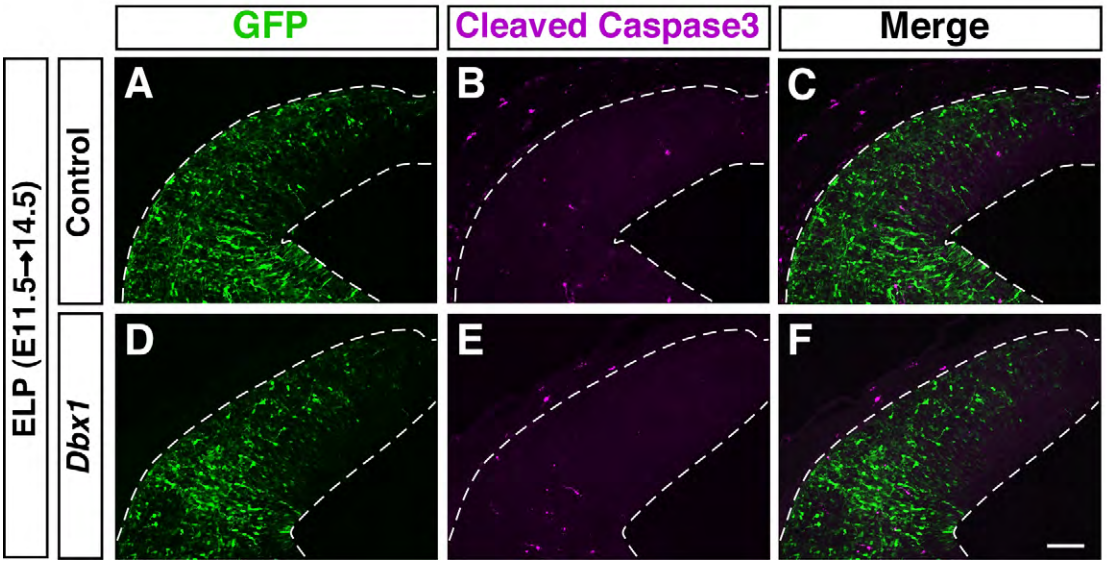

Fig. S7. Cell death analysis in Dbx1-misexpressed dorsal midbrain.

(A-F) Expression of cleaved caspase-3, a marker for detecting apoptotic cells, in the dorsal midbrain of electroporated embryos. Because the number of ipsilateral axons is dramatically reduced in *Dbx1*-electroporated embryos (Fig. 6), we examined whether the decrease in the ipsilateral axons is caused by an apoptotic cell death of ipsilateral neurons due to an effect of *Dbx1* electroporation. (A-C) Expression of cleaved caspase-3 in control embryos (*n*=3). GFP-expression vector was electroporated at E11.5, and immunohistochemistry for expression of cleaved caspase-3 was performed in transverse cryostat sections at E14.5. (D-F) Expression of cleaved caspase-3 in *Dbx1-ires-GFP* electroporated embryos (*n*=4). Note that few apoptotic cells are detected in the midbrain of *Dbx1*-electroporated embryos as well as in controls. Scale bar: 100 μm.

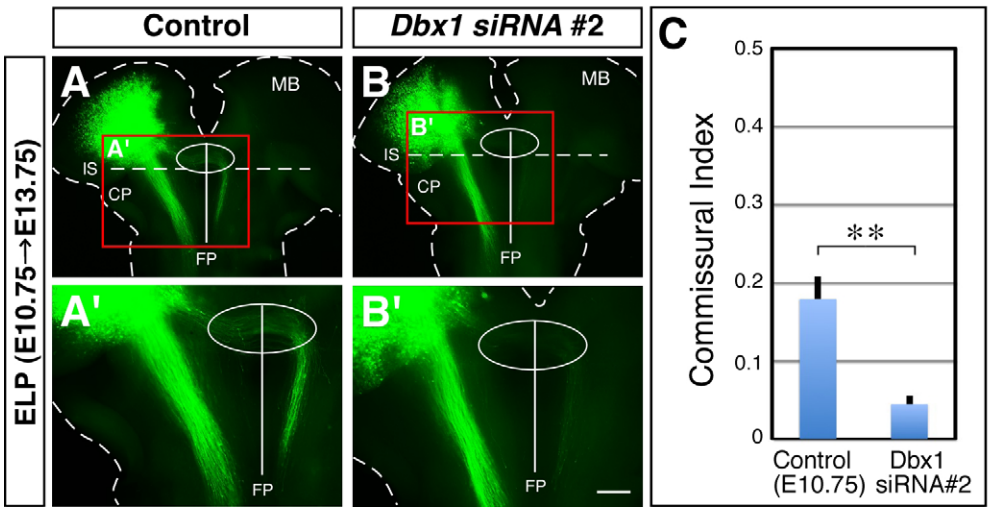

Fig. S8. Phenotype of Dbx1 knockdown using *Dbx1* siRNA (2nd target sequence).

(A,A') Trajectory of GFP-labeled axons in controls. *GFP* electroporation was performed at E10.75, and the electroporated brains were analyzed in flat-mounted preparations at E13.75 (*n*=8). Both commissural and ipsilateral axons are labeled. (B,B') Dbx1 knockdown using *Dbx1* siRNA (2nd target sequence) also results in loss of midline-crossing axons (*n*=7), similarly to that shown in Figure 6 (Fig. 6F,F'). Note that the target sequence used here is different from that employed in Figure 6. (A',B') Higher magnification views of red boxes in (A,B), respectively. (A-B') White oval indicate area around the ventral midbrain tegmentum that includes the floor plate (FP). (C) Quantification of midline crossing evaluated by commissural index (**P<0.01, Mann-Whitney U-test). Error bars indicate s.e.m. Scale bar: 500 μm in A,B; 250 μm in A',B'.

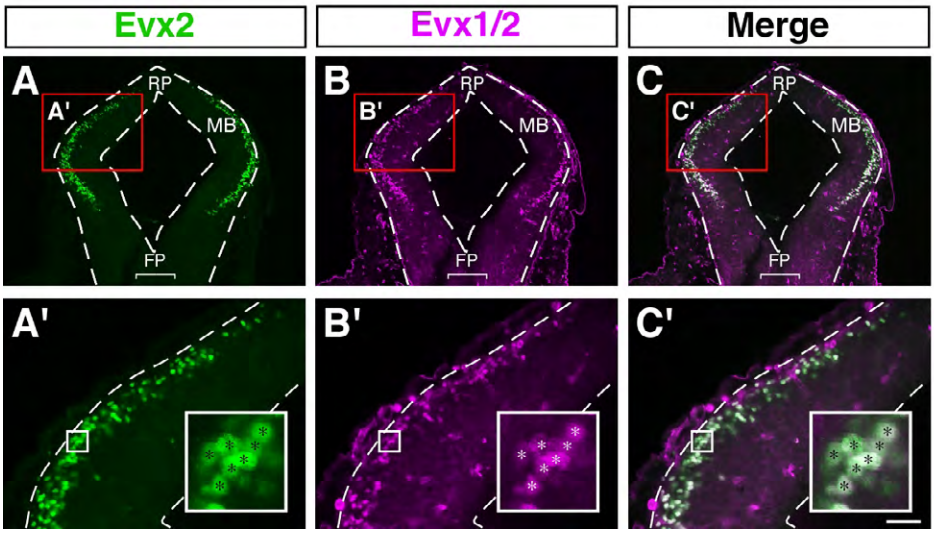

Fig. S9. Expression of Evx2 in the mouse midbrain.

(A-C') Expression of Evx2 in the dorsal midbrain at E11.5. (A'-C') Higher magnification views of red boxes in (A-C), respectively. Small boxes in (A'-C') indicate regions enlarged in insets. Asterisks in insets show that cells immunostained by polyclonal anti-Evx2 correspond precisely to those labeled by a monoclonal anti-Evx1/2 that detects Evx1 and Evx2 (Moran-Rivard et al., 2001, Neuron 29, 385-399; Pierani et al., 2001, Neuron 29, 367-384). Scale bar: 150 μm in A-C; 50 μm in A'-C'.

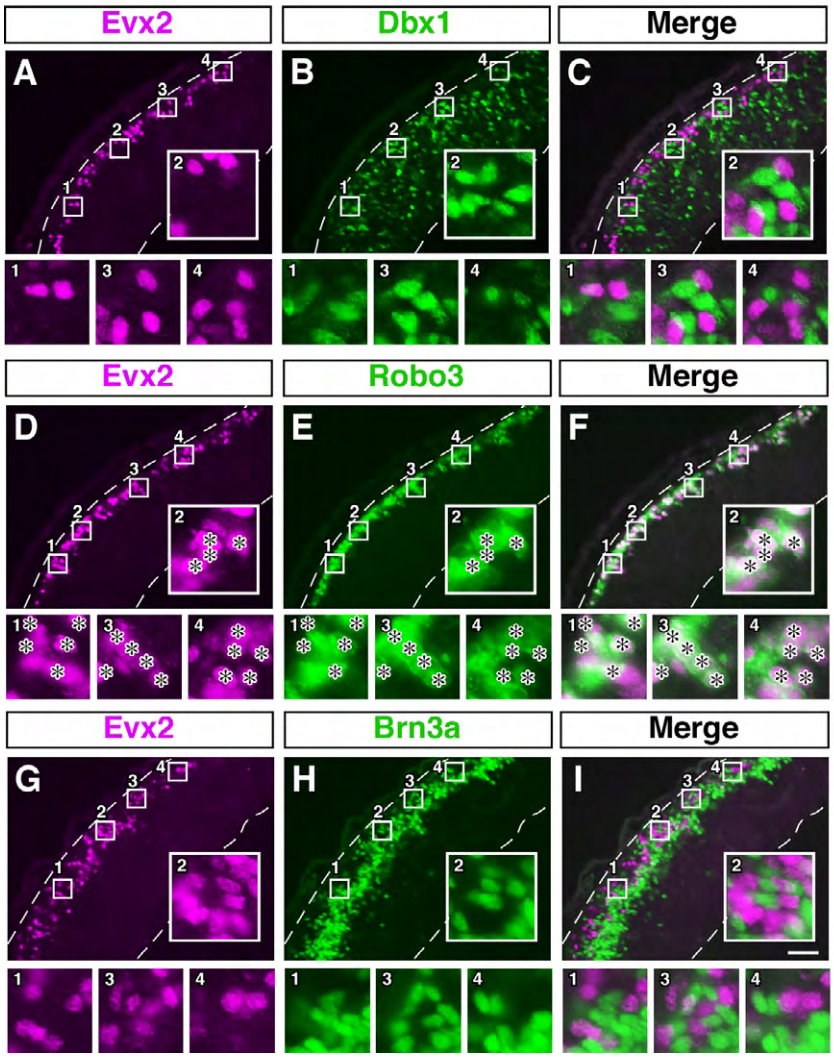

Fig. S10. Detailed expression analyses of Evx2 in the dorsal midbrain.

(A-I) Expression analyses of Evx2 by double-label immunohistochemistry in transverse sections of E11.5 dorsal midbrain. (A-C) Expression of Evx2 does not overlap with that of Dbx1. (D-F) Evx2-expressing cells correspond to Robo3-positive cells. Asterisks represent cells double-positive for Evx2 and Robo3 (insets). Because Robo3 is expressed not only in cell bodies but also on axons, some Robo3-positive/Evx2-negative areas are also observed. (G-I) Co-localization of Evx2 and Brn3a is not observed. Numbered small boxes in (A-I) indicate areas enlarged in corresponding insets below. Scale bar: 50 μm.

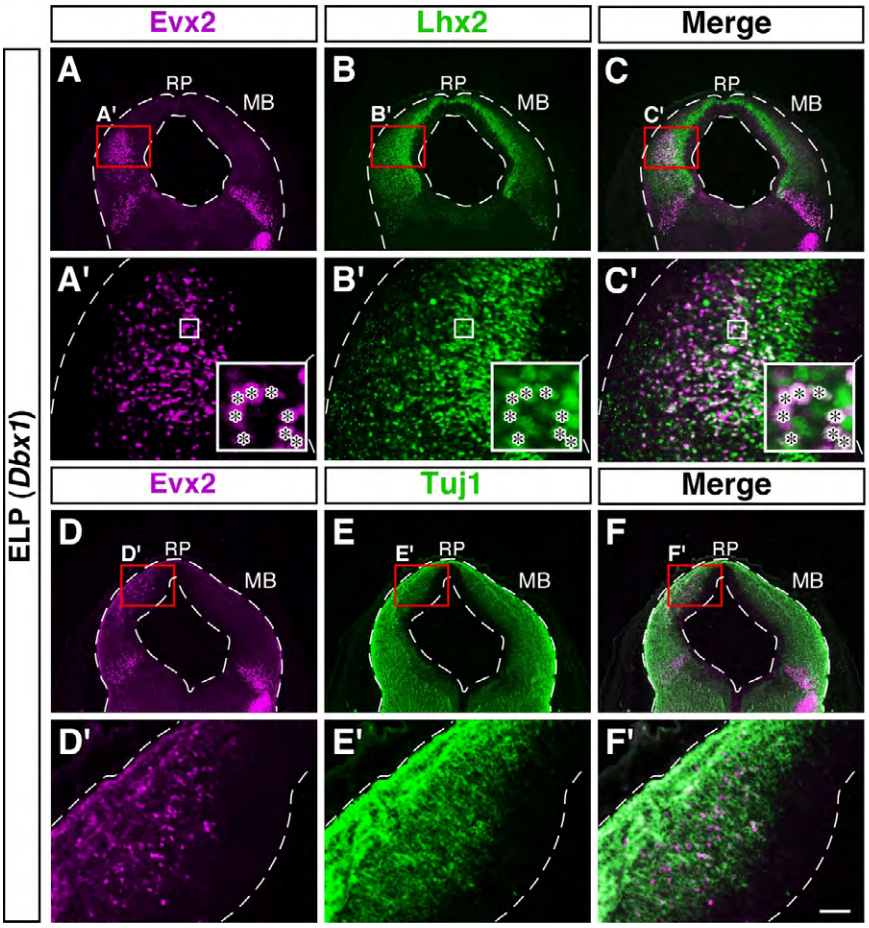

Fig. S11. Expression profile and the location of Evx2-positive cells induced by Dbx1 misexpression.

(A-C') Expression of Lhx2 in Evx2-positive cells that were ectopically induced by Dbx1-misexpression on the left side of the mid-brain. Electroporation of Dbx1-expression vector (without *ires-GFP*) was performed in E11.5 embryos (*n*=4), and the electroporated midbrains were subjected to double-label immunohistochemistry for expression of Evx2 and Lhx2 in transverse sections at E13.5. (A'-C') Higher magnification images of the red boxes in (A-C), respectively. Asterisks represent Evx2-positive cells that express Lhx2 (insets). Small boxes in (A'-C') indicate regions enlarged in insets. (D-F') Evx2-positive cells that were induced by Dbx1-misexpression are located in the postmitotic zone of the dorsal midbrain, as revealed by double immunolabeling of Evx2 and Tuj1 in transverse sections of E13.5 midbrain. Similarly to (A-C'), electroporation of *Dbx1* (without *ires-GFP*) was performed in E11.5 embryos (*n*=4). (D'-F') High power views of red rectangles in (D-F), respectively. Taken together, these results therefore suggest that Evx2-positive cells induced by Dbx1 misexpression undergo similar differentiation program as that operates in normal Evx2-expressing cells in wild type embryos. Scale bar: 250 µm in A-F; 50 µm in A'-F'.

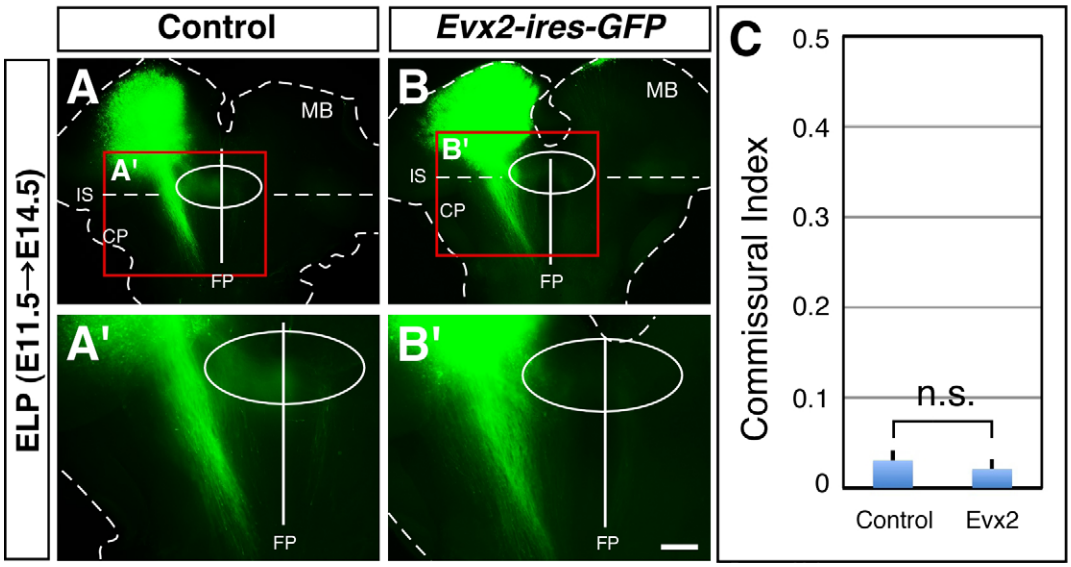

Fig. S12. Effect of Evx2 misexpression on the behavior of ipsilateral axons.

(A,A') Trajectory of GFP-labeled axons in controls. *GFP* electroporation was performed at E11.5, and the axonal trajectory was analyzed in flat-mounted preparations at E14.5 (*n*=10). The majority labeled by GFP are ipsilateral axons. (B,B') Electroporation of *Evx2 (Evx2-ires-GFP)* at E11.5 does not induce midline crossing (*n*=8), contrary to our expectations. We reason that, because Evx2 is a transcription factor normally started to be expressed at the postmitotic stage (Fig. 8), this phenotype may be caused by an atypical cellular context as a result of forced premature expression of Evx2 from the cycling progenitor stage by an electroporation-based gain-of-function approach. Indeed, it has recently been shown that the proper function of Barhl2, a postmitotically-expressed transcription factor that regulates the subtype diversification in the dorsal spinal cord, occurs only when Barhl2 is contextually expressed at the postmitotic stage (Ding et al., 2012, Proc. Natl. Acad. Sci. USA 109, 1566-1571). (A',B') Higher magnification views of red boxes in (A,B), respectively. (A-B') White oval indicate area around the ventral midbrain tegmentum that includes the floor plate (FP). (C) Quantification of midline crossing evaluated by commissural index. Error bars indicate s.e.m. Statistical significance was determined by Mann-Whitney U-test (n.s., not significant). Scale bar: 500 μm in A,B; 250 μm in A',B'.

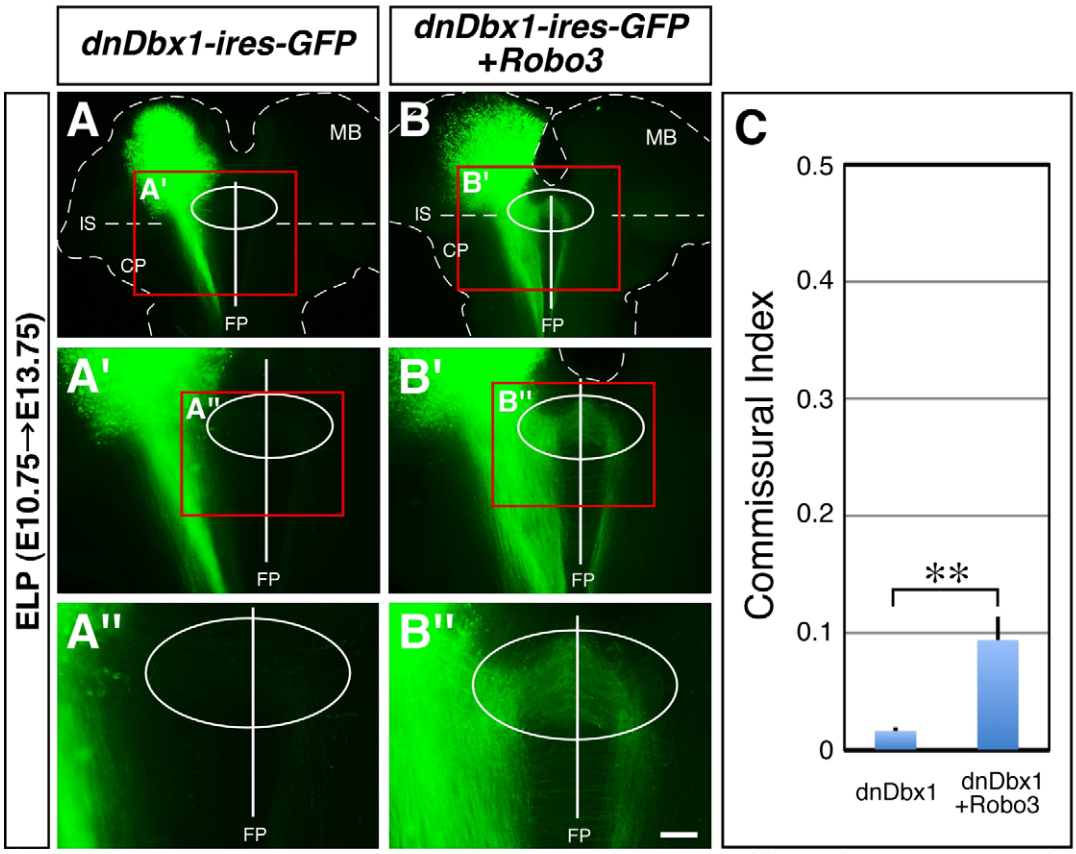

Fig. S13. Restoration of midline-crossing phenotype by Robo3 misexpression in the Dbx1 loss-of-function background.

(A,A',A") Axonal trajectory of *dnDbx1*-electroporated embryos. Electroporation of *dnDbx1* (*dnDbx1-ires-GFP*) was carried out at E10.75, and the effect on midline crossing was analyzed in flat-mounted preparations at 13.75 (*n*=8). Expression of dnDbx1 results in the absence of midline crossing (see also Fig. 6E,E'). (B,B',B") Midline-crossing phenotype is restored by an introduction of *Robo3* in *dnDbx1*-electroporated embryos (*n*=9). (A'-B") Higher magnification views of red rectangles in (A-B'), respectively. (A-G') White oval denotes area around the ventral midbrain tegmentum that includes the floor plate (FP). (C) Quantification of midline crossing evaluated by commissural index. Error bars indicate s.e.m. Statistical significance was determined by Mann-Whitney U-test (**P<0.01). Scale bar: 500 μm in A,B; 250 μm in A',B'; 125 μm in A",B".

Supplemental Table S1. Antibody List

Name	Source	Species	Dilution
Lhx2	Santa Cruz Biotechnology	Goat	1:300
Lhx9	Santa Cruz Biotechnology	Goat	1:100
Brn3a	Millipore	Mouse	1:600
Robo3	R&D Systems	Goat	1:160
Robo3	Tamada et al., 2008	Rabbit	1:500
Robo1	Tamada et al., 2008	Rabbit	1:1000
Tuj1	Covance	Mouse	1:1500
Ki67	BD Pharmingen	Mouse	1:200
Ngn1	Santa Cruz Biotechnology	Goat	1:400
Ascl1	BD Pharmingen	Mouse	1:600
ALCAM	R&D Systems	Goat	1:400
Evx1/2	DSHB	Mouse	1:50
Cleaved Caspase3	Cell Signaling Technology	Rabbit	1:600
GFP	Invitrogen	Rabbit	1:2000
GFP	Invitrogen	Chick	1:2000
ZsGreen1	TaKaRa	Rabbit	1:500